



A detailed experimental modal analysis of a clamped circular plate

David MATTHEWS¹; Hongmei SUN²; Kyle SALTMARSH²; Dan WILKES³; Andrew MUNYARD¹
and Jie PAN²

¹Defence Science and Technology Organisation, Australia

²University of Western Australia, Australia

³Curtin University, Australia

ABSTRACT

A detailed study has been made of the natural frequencies and modal shapes of a thin steel disc that is clamped at the edges by two steel flanges. The aim was to determine how accurately numerical modeling could be used to predict the results and to investigate the possibility of any new experimental observations even for this simple structure. A mechanical shaker and impact hammer were used to excite the plate to obtain the frequency response function of the structure. The first eight modal shapes at each of the resonant frequencies were then measured using laser scanning vibrometry. These results were compared with theoretical results obtained analytically and numerically using PAFEC. While part of the existing understanding of the plate vibration was confirmed, significant differences were found in the values of the modal frequencies. The experimental data also demonstrated a dependence of the mode shape orientations and splitting of degenerated natural frequencies on the shaker position and properties of the flanges. This paper will report on some interesting effects that need to be considered when doing such measurements and illustrate the risks of using numerical modeling without the use of experimental comparison.

Keywords: Modal Analysis, Clamped Edge Thin Plate, FEM, Laser Scanning Vibrometer I-INCE
Classification of Subjects Number(s): 21.4, 21.2.1, 75.6, 75.3, 75.5

1. INTRODUCTION

This work is part of a larger project involving the understanding of the near field acoustics of a submerged complex cylindrically shaped object. It is the initial attempt at benchmarking existing FEM with some experimental data from a very simple shape such as a clamped circular disk. Such a shape has been studied by a number of authors and has been well documented (1-9). If good agreement is found it provides encouragement that these models can be used for more complicated shapes.

2. EXPERIMENTAL SETUP

Figure 1a shows a schematic of the plate and flange configuration. It consists of a 1.6 mm steel plate with a radius of 290 mm and mass of 3.25 kg. This is rigidly clamped by two steel flanges with an outer radius of 290 mm and an inner radius of 206 mm. The mass of each flange is 31.80 kg. The two flanges are clamped together using ten 24 M steel bolts. The entire assembly was suspended from two steel eyes that were free to rotate when under load. The structure was attached to a wooden hanging frame using four rubber springers. A photograph of the disc is shown in figure 1b.

To excite the structure a B&K 4810 mini shaker was attached on the centerline of the disc and at a distance of 145 mm from the center. Attachment was made via a B&K 8001 force impedance head which was attached to the steel disc using a strong magnetic stud. The shaker was driven by a HP

¹ david.matthews@dsto.defence.gov.au

² hongmei.sun@uwa.edu.au

³ daniel.wilkes@postgrad.curtin.edu.au

8904A signal generator. The signal was amplified using a B&K 2704 power amplifier to provide an adequately large signal to shake the assembly. A PCB 352C67 accelerometer was placed at a distance of 125 mm from the center of the disc and at an angle of 52° from the vertical. A photograph of the assembly is shown in figure 1b. The shaker was held in position using a pulley system to minimize mass loading effects. It was possible to move the shaker to any position required on the face of the assembly. In addition to the shaker the disk was also excited using a B&K 8206 impact hammer and a non-contact electromagnetic exciter.

The frequency response function was measured for the first 1000 Hz using white noise. Data acquisition was made using a B&K Pulse system with a frequency resolution of 1 Hz. A Polytec scanning laser doppler velocimeter (SLDV) was then used to scan the front of the disk at each of the first eight modal frequencies.

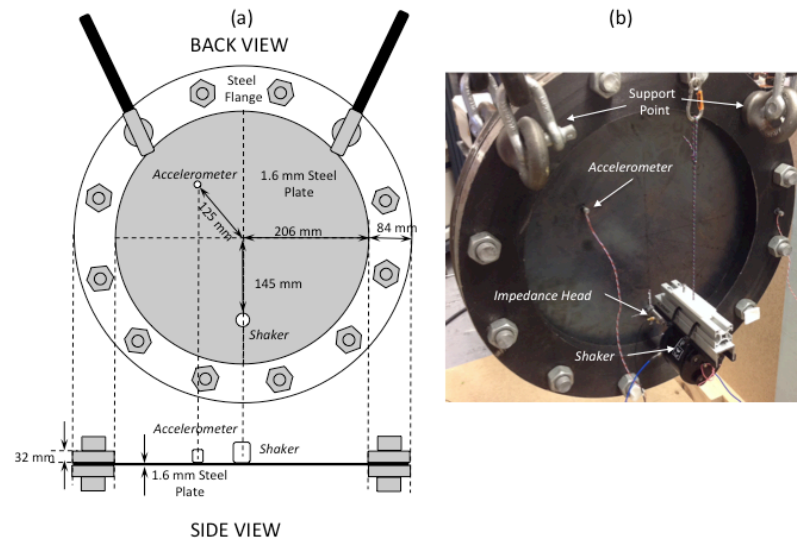


Figure 1. Clamped disc setup

3. RESULTS

Figure 2 shows the experimental frequency variation of the drive point accelerance and test point accelerance for the first 1000 Hz. An initial attempt to model the clamped disk was done analytically using standard Kirchoff-Love plate theory (4). For the analytical model the following parameters were used; Young's modulus (Q) = 210 GPa, Poisson's ratio (ν) = 0.3, density (ρ) = 7872 Kg m^{-3}

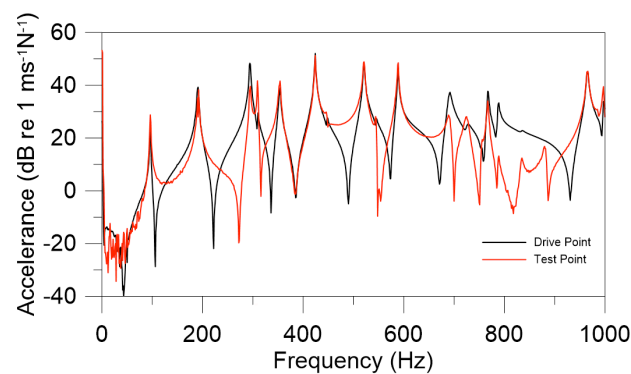


Figure 2. Frequency response function (FRF) for drive point accelerance and test point accelerance.

Table 1 shows a comparison of the measured frequencies with the analytical values. The first column shows the results obtained using the B&K mini shaker. This was the main method used to shake the structure in this paper. The second two columns are experimental results obtained using two different excitation methods. These will be discussed later in the paper. Comparison of the mini shaker results to the theory shows good agreement for the first two frequencies after which the fit deteriorates. For classical plate theory the boundary is assumed to be rigidly clamped and the effect of the flanges are not considered. As a result all calculated modal frequencies are associated with the disc alone. FEM however can model the entire structure including the flanges, bolts and support eyes. These calculations were done using PAFEC (10) using the same physical parameters as the analytical model. The results are shown in Table 1. As can be seen there is very good agreement between the analytical model and PAFEC. This is surprising considering that PAFEC has taken into account a detailed model of entire flange structure. However they are both significantly higher than the experimental results especially at higher frequencies. It is also interesting that theoretically the (2,2) mode at $f \sim 792$ Hz lies between the (4,1) and the (0,3) mode. Experimentally no peak lies between these two modes. In order to try and explain these differences the effects of shaker position, shaker mass and flange tightness was investigated. The two frequencies shown in brackets in Table 1 are from the same mode and their origin will be discussed below.

Table 1. Comparison of experimental modal frequencies to those obtained using classic plate theory and FEM.

Experiment Mini Shaker	Experiment Impact	Experiment EM Shaker	Classic Plate Theory		PAFEC
Frequency (Hz)	Frequency (Hz)	Frequency (Hz)	(m,n)	Frequency (Hz)	Frequency (Hz)
97	94	97	(0,1)	96	96
191	(188, 192)	195	(1,1)	199	199
(296, 312)	(303, 310)	(308, 312)	(2,1)	327	326
355	356	361	(0,2)	373	373
(426, 450)	(441, 449)	447	(3,1)	479	478
511	-	-	Flange	-	600
547	(537, 543)	542	(1,2)	571	570
590	608	612	(4,1)	653	653
-	-	-	(2,2)	793	792
695	740	749	(0,3)	836	835

3.1 Effect of the steel flanges

To investigate the frequency response of the steel flanges two accelerometers were attached to the flange. One was placed on the face of the flange to measure any movement perpendicular to the disc and the other on the edge to measure any radial vibration. An impact hammer was used to excite the structure by either striking perpendicular or radially to the flange. Figure 3 shows the FRF for the steel plate (blue), the transverse response of the flange (red) and the radial response of the flange (black). For the transverse response a peak was measured at 512 Hz and for the radial one at 1117 Hz. A comparison of the FRF shown in Figure 2 clearly shows a peak around 512 Hz which is in good agreement with the peak detected on the flange using the impact hammer.

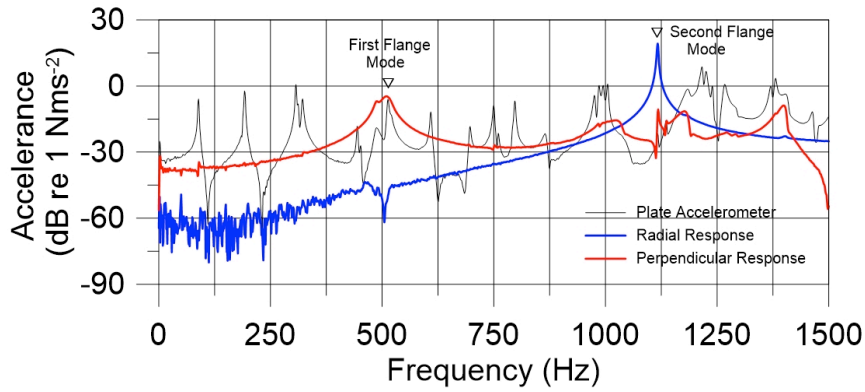


Figure 3. Perpendicular and radial frequency response curve for the flange

3.2 Modal shapes and identification

In order to identify various modes with the observed peaks in the FRF in Figure 2, a 1D laser scanning vibrometer (PSV-400, Polytec) was used to scan the structure at each of the measured resonant frequencies. The vibrometer uses a user defined grid to measure the time signal of the response of the structure which is being excited by the shaker on the opposite side. The measurement grid on the plate consisted of 409 points resulting in a grid spacing of 0.022 m. The same spacing was used for the flange. Since the flange and plate are perpendicular to the laser the results give a good measure of the velocity normal to the surfaces. This was done both for the plate and the flange. In order to excite the flange the shaker was moved and attached directly to the flange face. The results are shown in Figure 4.

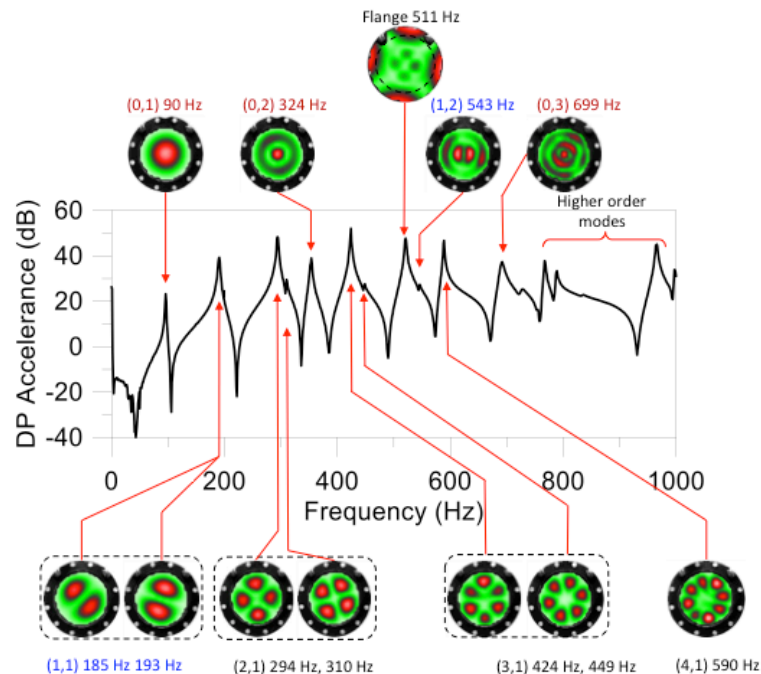


Figure 4. Modal shapes for all measured resonant frequencies below 700 Hz

As can be seen all the resonance peaks have been successfully identified with their associated mode shapes. The peak at 511 Hz has been confirmed as being the first flange mode as was suggested

by the impact hammer measurements above. It was not possible to confirm the second flange mode at 1117 Hz as this is a radial mode and the laser vibrometer only measures displacements normal to the surface. It is interesting to note how all of the asymmetric mode peaks in Figure 4 ((1,1),(2,1) and (3,1)) have a small side peak at slightly higher frequency. These frequencies have been shown in brackets in Table 1. Laser scans at both frequencies revealed that they are both associated with the same mode except 90° out of phase. This is predicted from the theory but at the same frequency. One possible explanation is that it is due to variations in the boundary condition between the plate and the flange. All the bolts were uniformly tightened but the two suspension points were free to rotate when placed under tension. As a result the stress fields in the vicinity of the suspension points would probably be lower than in the rest of the flange resulting in an asymmetry of the structural resonances. Another possibility is that it is due to the mass loading effect of the shaker. These will be discussed below.

3.3 Effect of shaker position on Modal shapes

For all laser scans shown in Figure 4 the shaker was positioned on the center line of the disc as shown in Figure 1. Inspection of the asymmetric mode shapes shows the maxima of the (2,1) and (3,1) aligning with shaker position, however, the (1,1) mode lies approximately at an angle of 20° to the vertical for the shaker in the original position. To investigate the effect of the shaker on the orientation of the asymmetric modes the shaker was moved at a constant radius of 145 mm and positioned every 10° in an anticlockwise direction looking from the back. The FRF was measured at each position using white noise and the asymmetric mode shape measured using a laser vibrometer. The result are shown in Figure 5a and 5b for the (1,1), (2,1) and (3,1) modes.

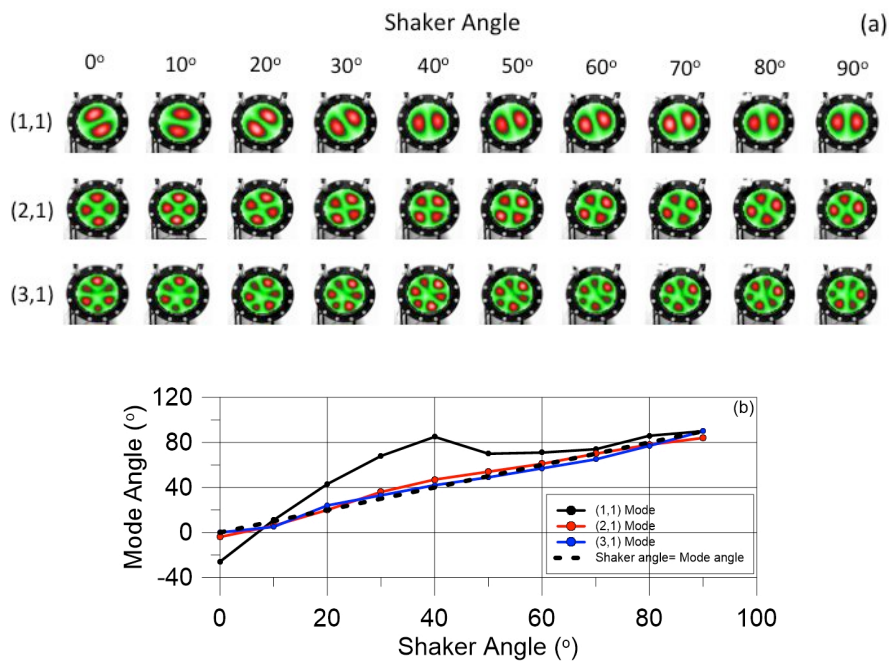


Figure 5. Effect of shaker position on the asymmetric mode shapes.

There is good agreement between the shaker position and the angle of the mode shape for both the (2,1) and (3,1) modes for the entire range of positions. The correlation however is not as good for the (1,1) mode. Theoretical results done with PAFEC are shown in Figure 6. They clearly show the mode shape following the shaker position. Due to computation limitations results were only generated for $\theta = 0^\circ, 20^\circ, 40^\circ$ and 60° . The experimental model frequencies used to obtain Figure 5 were also used for the PAFEC results shown in Figure 6. Inspection of Table 1 shows that for the (1,1) and (2,1) modes the experimental and theoretical values are reasonably close. For the (3,1) however the difference is more significant. As a result the driving frequency used for the (3,1) mode in PAFEC might be too far away from the predicted modal frequency and the mode shape may not be fully

formed. This would explain the differences in mode shapes observed for the (3,1) mode in Figures 6. Despite this the theoretical results clearly show the mode shape closely following the shaker position even for the (1,1) mode. The anomalous experimental results observed for the (1,1) mode could possibly be due to the asymmetries in the boundary conditions do to the support points.

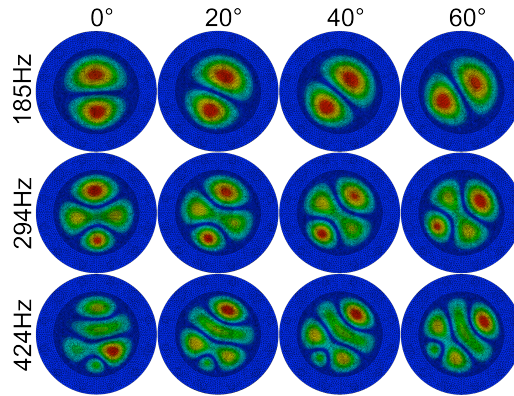


Figure 6. Theoretical results for the mode shift as a function of shaker position for the (1,1), (2,1) and (3,1) modes

3.4 Mass loading effect of the shaker

To investigate the mass loading effect of the shaker two alternative excitation methods were used to drive the disc. One was an impact hammer and the other an electromagnet. Both were used to excite the disc at the same point as the mini shaker. The electromagnet provides a non-contact method to excite the disc thus eliminating any mass loading effects that could be introduced with mini shaker. The drawback of this system is the lack of information about the input force required for calculating the mobility of the structure. By using white noise it was possible to achieve broadband excitation of the disc and record the spectrum of the test accelerometer. The result is shown in red in Figure 7. The peak positions have been indicated in the same color. As a comparison an impact hammer was also used to measure the drive point acceleration (blue curve in Figure 7) and both of these have been compared to the drive point acceleration using the mini shaker (black curve in Figure 7).

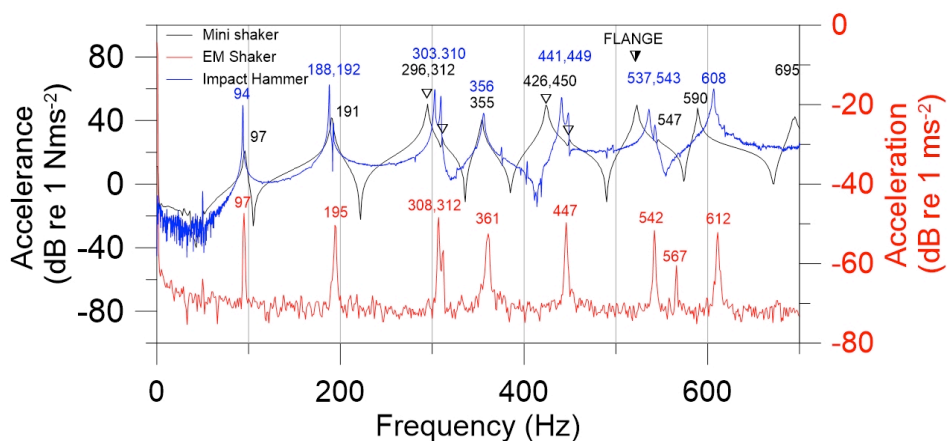


Figure 7. Effect of mini shaker on the experimental modal frequencies of the structure

The first three columns in Table 1 show all the measured frequencies found in Figure 7. It is clear that the mini shaker decreases all the frequencies and the difference becomes larger at higher frequencies. For the (2,1) and the (3,1) modes two distinct peaks were found associated with the same mode. These have been indicated by black triangles in the figure. As the mass loading effect is

reduced by using the impact hammer and EM shaker, the difference in frequency becomes less and even reduces to a single line for the (3,1) using the EM shaker. The converging frequency ends up being the larger of the original two obtained using the mini shaker. This suggests that the mass loading effect of the mini-shaker introduces an asymmetry in the disc causing two distinct frequencies for the same mode. Any remaining closely spaced double peaks observed with the non-contact shaker are most likely due to imperfections in the plate and flanges themselves.

3.5 Effect of boundary conditions

As mentioned above the steel disc is clamped on each side by two steel flanges. These flanges have ten M24 bolts and two support eyes holding them in place. To investigate the effect of the clamping on the modal frequencies each bolt was tightened to a certain torque and the frequency response of the test accelerometer measured. Due to SNR issues the disc was excited using the mini shaker and as a result the measured modal frequencies will be lower than those obtained using a non-contact shaker. Torque values ranging from 6 Kgm to 15 Kgm were measured and the effect on the frequency of the first nine modes (including the flange) recorded. The results are shown in Figure 8. It is clear that increasing the bolt tightness results in an increase in the frequency of each mode. For the lower order modes this increase is in the order of a few Hertz but for the higher order modes it can be as large as 30 Hz. Such sensitivity to the clamping conditions were also reported by Kung (3). Logarithmic curves were fitted to the limited data and the results are shown on each plot in Figure 8. Due to the setup of the experiment the maximum possible torque achievable was 15 Kgm. It was also difficult to accurately adjust the torque setting for each bolt due to frictional effects.

In order to estimate the increase in frequency that can be expected using higher torques the fits obtained in Figure 9 were used to calculate the resulting frequencies for a torque of 50 Kgm. It was hoped that this would give a better approximation of a truly clamped disc which is what the analytical model and PAFEC assume in their calculation. The results are shown in column 3 of Table 2. Column 3 shows the effect of mass loading of the mini shaker compared to the non-contact shaker. Inspection of the (2,1) and (3,1) mode double peaks show that both frequencies are shifted up with a decrease in mass loading. In the case of bolt tension the second peak remains stationary. After correcting for the effects of mass loading and bolt tension the resulting modal frequencies agree much better with PAFEC than the original frequencies (see column 5). For frequencies greater than the (1,2) mode frequency however there is still some significant differences.

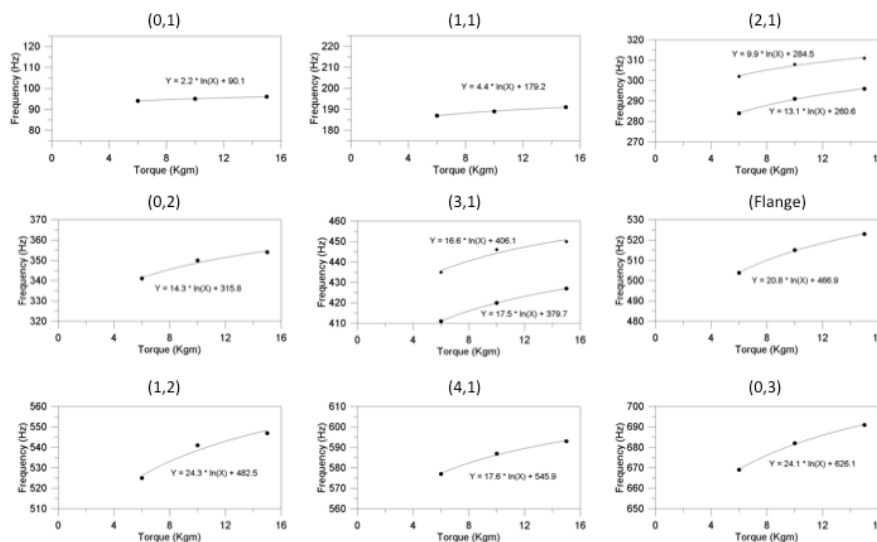


Figure 8. Effect of bolt tension on the first nine modal frequencies

Table 2. Effect of mass loading and flange tension on the experimental modal frequencies

MODE (m,n)	Mode Frequency Original (Hz)	Mass Loading Correction (Hz)	Clamping Correction (Hz)	Corrected Frequency (Hz)	PAFEC Frequency (Hz)
(0,1)	97	0	2	99	96
(1,1)	191	4	5	200	199
(2,1)	(296, 312)	(12, 0)	(18, 11)	326, 323	326
(0,2)	355	6	17	378	373
(3,1)	(426, 450)	(21, 0)	(22, 21)	469, 471	478
	511		37	548	600
(1,2)	547	-5	31	573	570
(4,1)	590	22	25	637	653
(2,2)	-	-	-	-	792
(0,3)	695	54	25	774	835

4. CONCLUSIONS

A detailed experimental modal analysis of a clamped, thin circular plate has been made and the results compared to theory. Using a scanning laser vibrometer it was possible to identify the first eight modal frequencies with their corresponding mode shapes. In addition to the disc modes two flange modes were also identified. It was found that results agreed well at lower frequencies with theoretical results using classical plate theory and PAFEC but that significant differences were found at higher frequencies. Some of these difference can be attributed to the mass loading of the shaker and the effects of the boundary clamping force.

The measured modal frequencies are sensitive to mass loading and boundary condition effects. Mass loading reduces the modal frequencies with shifts of up to 50 Hz observed at higher order modes. Lower order modes were less affected. Increasing the boundary clamping force resulted in an increase in the modal frequencies. This is expected as the net result is the achievement of the perfect boundary condition where there is zero displacement and zero bending rotation. For the modal analysis using PAFEC this is what is assumed. Attempts at correcting for these two effects gives improvements in the agreement with PAFEC although there are still some significant differences at higher frequencies. Incorporating static applied pressures when doing the modal analysis would result in a more realistic model. This will be considered for further work.

The position of various modes is strongly influenced by the position of the shaker. The (2,1) and the (3,1) modes follow the shaker position very closely. The (1,1) mode however shows less dependence especially at angles less than 70°. While this mode position does have some correlation with the shaker position it appears that there also some addition influence such as the asymmetric boundary clamping force imposed by the eye supports. Why this mode is more sensitive to such things is unclear at this stage. Theoretical results using PAFEC showed that the mode positions follow the shaker position.

At various shaker positions the asymmetric modes ((1,1), (1,2), (1,3)) clearly show two peaks associated with the same mode. Theoretically these two orthogonal modes should occur at a single frequency but differences as large as 50 Hz were observed. It was shown that this was mainly due to the mass loading effect of the shaker. Use of a non-contact shaker showed either just a single peak or two very close together. In both cases the modal frequency was shifted up to the upper peak position found using the contact shaker results. Observation of a double peak in the non-contact modal frequencies is most likely due to imperfections in the plate and flanges themselves.

Analytical and computational models need to be used carefully when making predictions about the modal frequencies even for a simple structure such as the one discussed in this paper. Predictions for complex structures should not be done without careful experimental validation.

REFERENCES

1. Leissa AW. *Vibration of Plates*. Washington : Scientific and Technical Information Division, National Aeronautics and Space Administration, 1969. p.7-35
2. Hansen CH and Bies DA. Optical holography for the study of sound radiation from vibrating surfaces. *J Acoust Soc Am*, 1976;60(3): 543-555.
3. G.C Kung and Y.H Pao. Non-linear flexural vibrations of a clamped circular plate. *Journal of Applied Mechanics*, pages 1050–1054, 1972.
4. Morse PM. *Vibration and Sound*. American institute of physics, third edition, 1981. p. 183-213.
5. Fahy F and Gardonio P. *Sound and Structural Vibration*. Academic Press, second edition, 2007.
6. Soedel W. *Vibration of Shells and Plates*. CRC Press, third edition, 2005.
7. A Lurie. *Theory of Elasticity*. Springer, first edition, 2005.
8. L. D Landau and E. M Lifshitz. *Theory of Elasticity*. Elsevier, second edition, 1986.
9. S Timoshenko and S Woinowsky-Krieger. *Theory of plates and shells*. McGraw-Hill College, second edition, 1959
10. PACSYS:FEA / BEM Solutions; 2014. Available from: <http://www.vibroacoustics.co.uk/>.